tion-metal ions with alkanes. This difference in reactivity is attributed to the thermodynamically less demanding process of generating silylene from the silanes compard to carbene formation from the corresponding alkanes. Metal–silylene bond dissociation energies, estimated by examining the reaction thermochemistry associated with metal silylene formation, are stronger for Co^+ and Ni^+ than for the other metal ions. The bonding between transition-metal ions and silylene is described by σ-donation of nonbonding lone-pair electrons from the ground-state silylene to the metal center, and π-back-donation of paired 3d electrons from the metal into the empty 3p orbital of Si is invoked to account for the strengthened Ni^+–SiH_2 and Co^+–SiH_2 bonds.

Acknowledgment. We gratefully acknowledge the support of the National Science Foundation under Grants CHE 8407857 (J.L.B.) and CHE 8512711 (M.T.B.). Graduate fellowship support by the Korean Government (H.K., 1980–1984) is gratefully acknowledged.

Registry No. Ni^+, 14903-34-5; Co^+, 16610-75-6; Fe^+, 14067-02-8; Cr^+, 14067-03-9; V^+, 14782-33-3; Ti^+, 14067-04-0; SiH_4, 7803-62-5; SiH_3Me, 992-94-9; SiH_2Me_2, 1111-74-6; $SiHMe_3$, 993-07-7; $SiMe_4$, 75-76-3; Si_2Me_6, 1450-14-2.

Activation of Alkanes by Ruthenium, Rhodium, and Palladium Ions in the Gas Phase: Striking Differences in Reactivity of First- and Second-Row Metal Ions

M. A. Tolbert, M. L. Mandich, L. F. Halle, and J. L. Beauchamp*

Contribution No. 7380 from the Arthur Amos Noyes Laboratory of Chemical Physics, California Institute of Technology, Pasadena, California 91125. *Received March 14, 1986*

Abstract: The reactions of Ru^+, Rh^+, and Pd^+ with alkanes are studied in the gas phase by using an ion beam apparatus. The reactivity of the second row group 8–10 metal ions is shown to be dramatically different than that of their first-row congeners. Studies with deuterium labeled alkanes reveal that Ru^+, Rh^+, and Pd^+ all dehydrogenate alkanes by a 1,2-mechanism, in contrast to the 1,4-mechanism of Co^+ and Ni^+ and the combination of 1,2- and 1,4-processes for Fe^+. In most respects, Ru^+ and Rh^+ exhibit similar reactivity quite distinct from that observed for Pd^+. The reactions of Ru^+ and Rh^+ are dominated by the loss of one or more molecules of hydrogen, via mechanisms characterized by C–H bond insertions and β-H transfers. In contrast to the reactions of their first-row congeners, neither β-methyl transfers nor C–C bond insertions occur competitively at Ru^+ and Rh^+ centers. Furthermore, evidence is presented which indicates that the barriers for reductive elimination of H_2 and HR from Rh–(olefin)$^+$ complexes are much smaller than the corresponding barriers for the first row group 8–10 metal ions. These low barriers may result in the formation of internally excited products able to undergo a second exothermic elimination reaction. The differences in reactivity of the first and second row group 8 and 9 metal ions are proposed to be due to differences in the sizes and shapes of the orbitals used for bonding. Although the reactivity of Pd^+ appears in some ways to be quite similar to that of Ni^+, the mechanism by which alkanes are activated by Pd^+ may be quite different than for any of the first-row metal ions. It is proposed that the uniquely high Lewis acidity of Pd^+ results in hydride abstraction as a first step in the mechanism for C–H bond activation, leaving the hydrocarbon fragment with an appreciable amount of carbonium ion character in the reaction intermediate. This mechanism is supported by the fact that Pd^+ dehydrogenates *n*-butane by a 1,2-elimination across the central C–C bond exclusively. Palladium is the only metal ion studied to date which undergoes this selective elimination.

The determination of the mechanism by which alkanes are activated by transition-metal ions in the gas phase is an intriguing and challenging problem. The reaction mechanisms are necessarily complex, multistep processes. Furthermore, the reactions often result in the formation of many products. Fundamental for understanding the mechanisms of these reactions is a knowledge of the activation parameters for competing processes. What factors control C–C vs. C–H bond insertion? What determines the relative rates for β-hydrogen vs. β-alkyl transfers?

Clues to the puzzle of hydrocarbon activation by transition-metal ions have been obtained by using a variety of complementary techniques. The studies to date include the reactions of the entire first-row transition-metal series and several metal ions in the second-row series.[1-6] Ion beam and ion cyclotron resonance (ICR) techniques have been used successfully to identify the products of these reactions and to obtain thermochemical information. In addition, recent studies of product translational energy release distributions have probed the potential energy surfaces for elimination of H_2 and small hydrocarbons from ionic iron, cobalt, and nickel complexes.[7,8] By the use of these complementary tech-

Table I. Homolytic and Heterolytic Bond Dissociation Energies for Group 8–10 Transition-Metal Ions in the Gas Phase

	bond dissociation energy (kcal/mol)					
	Fe	Co	Ni	Ru	Rh	Pd
M^+–H	53[a]	48[a]	39[a]	41[b]	42[b]	45[b]
M^+–CH_3	68[b]	61[c]	48[c]	54[b]	47[b]	59[b]
M^+–H^-	208[d]	218[d]	224[d]	208[d]	214[d]	231[d]

[a] Reference 10. [b] Reference 11. [c] Reference 32. [d] Reference 13.

(1) (a) Armentrout, P. B.; Beauchamp, J. L. *J. Am. Chem. Soc.* **1981**, *103*, 784. (b) Halle, L. F.; Armentrout, P. B.; Beauchamp, J. L. *Organometallics* **1982**, *1*, 963. (c) Houriet, R.; Halle, L. F.; Beauchamp, J. L. *Organometallics* **1983**, *2*, 1818.

(2) (a) Allison, J.; Freas, R. B.; Ridge, D. P. *J. Am. Chem. Soc.* **1979**, *101*, 1332. (b) Larson, B. S.; Ridge, D. P. *J. Am. Chem. Soc.* **1984**, *106*, 1912.

(3) (a) Byrd, G. D.; Burnier, R. C.; Freiser, B. S. *J. Am. Chem. Soc.* **1982**, *104*, 3565. (b) Jacobson, D. B.; Freiser, B. S. *J. Am. Chem. Soc.* **1983**, *105*, 5197.

(4) Tolbert, M. A.; Beauchamp, J. L. *J. Am. Chem. Soc.* **1984**, *106*, 8117.

(5) Byrd, G. D.; Freiser, B. S. *J. Am. Chem. Soc.* **1982**, *104*, 5944.

(6) Carlin, T. J.; Jackson, T. C.; Freiser, B. S., to be submitted for publication.

(7) (a) Hanratty, M. A.; Beauchamp, J. L.; Illies, A. J.; Bowers, M. T. *J. Am. Chem. Soc.* **1985**, *107*, 1788. (b) Hanratty, M. A.; Beauchamp, J. L.; Illies, A. J.; Bowers, M. T., submitted to *J. Am. Chem. Soc.* for publication.

0002-7863/86/1508-5675$01.50/0

niques, a more complete picture of hydrocarbon activation processes is emerging.

In this paper, we describe the reactions of three second-row metal ions, Ru^+, Rh^+, and Pd^+, with saturated hydrocarbons in the gas phase. We find that the reactivity of these metal ions is dramatically different than that of their first-row congeners. From an understanding of these differences, we gain a better understanding of hydrocarbon activation by first row as well as second-row transition-metal ions.

The first step in a comparison of the differences between the first- and second-row metal ions has been made in previous studies of the binding energies of H and CH_3 to transition-metal ions.[1b,9-11] These results are presented in Table I for the first and second row group 8–10 metal ions. Also included in this table are recently determined heterolytic M^+–H^- bond energies.[12,13] These bond dissociation energies are useful to interpret mechanistic differences in comparing the reactivity of first- and second-row transition-metal ions with alkanes.

Experimental Section

The ion beam apparatus used in the present study has been described previously.[14] Briefly, ion beams of Ru^+, Rh^+, and Pd^+ are produced by vaporization of $Ru_3(CO)_{12}$, $[Rh(CO)_2Cl]_2$, and $PdCl_2$(anhydrous) onto a hot rhenium filament and subsequent surface ionization at 2500 K. In this experimental arrangement, electronically excited ions are less than 1% of the total ion abundance for Ru^+, Rh^+, and Pd^+.[11] The metal ions are collimated, mass and energy selected, and focussed into a collision chamber containing the neutral reactant at ambient temperature. Product ions scattered in the forward direction are analyzed by using a quadrupole mass spectrometer.

The exothermic reactions of Rh–(olefin)$^+$ complexes were studied by using the above apparatus equipped with a dual inlet system which allowed independent addition of two reagent gases. Rhodium ethylene and propylene complexes were formed by reaction with ethane and propane as indicated in eq 1 and 2, respectively. Loss of H_2 is the only exothermic process observed in these reactions. Further reactions of the olefin complexes were studied by adding an equal pressure of a second reactant gas to the collision chamber and observing the new products formed. The total pressure of reagent gas was held constant at 4 mtorr. Under these conditions, most of the rhodium ions suffer approximately two collisions. If the first collision results in the exothermic formation of Rh(olefin)$^+$, a second collision may result in further reaction of the metal–olefin complex. In order to observe only exothermic reactions, the relative kinetic energy used in these experiments was quite low, <0.25 eV.

$$Rh^+ + C_2H_6 \rightarrow Rh(C_2H_4)^+ + H_2 \quad (1)$$

$$Rh^+ + C_3H_8 \rightarrow Rh(C_3H_6)^+ + H_2 \quad (2)$$

Labeled ethane (*1,1,1-d_3*, 98% D), propane (*2,2-d_2*, 98% D), *n*-butane (*1,1,1,4,4,4-d_6*, 98% D), and 2-methylpropane (*2-d_1*, 98% D) were obtained from Merck, Sharp and Dohme.

Results

The second row group 8, 9, and 10 metal ions are all observed to react with alkanes resulting in a wide variety of products. As an example, consider the reaction of Rh^+ with *n*-butane. The reaction cross sections as a function of relative kinetic energy are shown in Figure 1. The exothermic products are easily identified since their reaction cross sections decrease with increasing relative kinetic energy as indicated in Figure 1a. The results of reacting Co^+ with *n*-butane are also illustrated in Figure 1 for comparison.[1a] It can be seen that there are significant differences in product distributions and their variation with translational energy in the reactions of Co^+ and Rh^+ with *n*-butane. Whereas Co^+ reacts to form three exothermic products corresponding to loss of H_2, CH_4, and C_2H_6, only hydrogen loss products are observed as exothermic reactions for Rh^+. The alkane loss channels for Rh^+ appear to have translational energy thresholds, as indicated in Figure 1b.

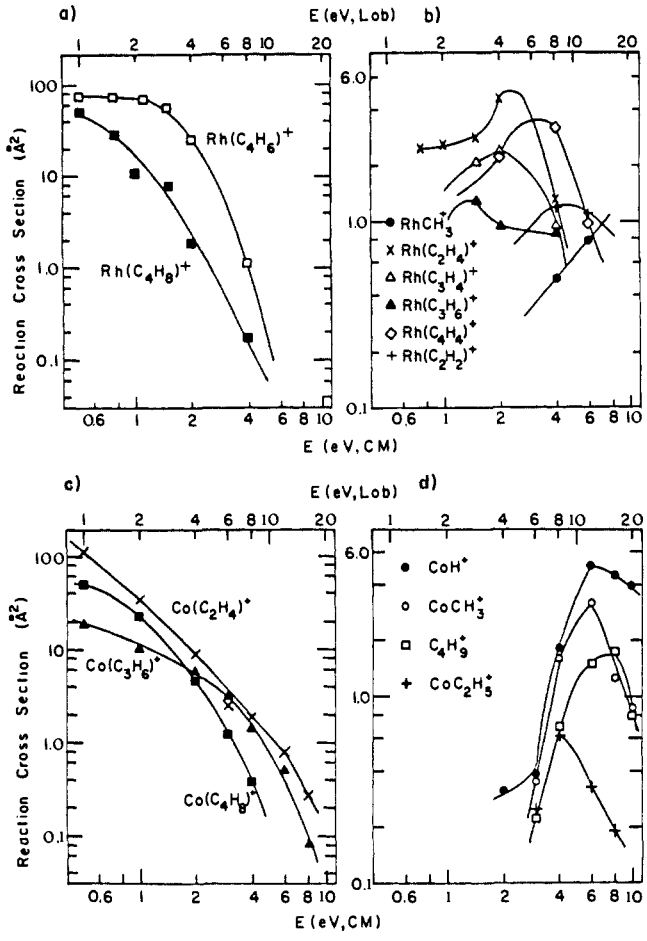

Figure 1. Variation in the experimental cross section for the (a) exothermic reactions and (b) endothermic reaction of Rh^+ with *n*-butane as a function of relative kinetic energy and for the (c) exothermic reactions and (d) endothermic reactions of Co^+ with *n*-butane as a function of relative kinetic energy, ref 1a.

Product distributions and overall cross sections for the reactions of alkanes with Ru^+, Rh^+, and Pd^+ at a relative kinetic energy of 0.5 ev are given in Table II. Also included in this table are previous ICR results for the exothermic reactions of Rh^+ with alkanes.[5] It can be seen that, although the results of the ion beam experiment agree fairly well with the ICR data, there are some noteworthy discrepancies in several cases. The ICR experiments utilized rhodium ions that were produced by laser evaporation of a metal target or by electron impact ionization of $(\eta^5\text{-}C_5H_5)Rh(CO)_2$. Electron impact ionization has been shown to produce a distribution of ground- and excited-state metal ions.[11,15,16] Recent studies have also shown that metal ions created by laser evaporation are formed with a wide distribution of translational energy and may be electronically excited as well.[17]

From our examination of product distributions as a function of relative kinetic energy, it appears that most of the deviations of our results from earlier ICR measurements can be explained by assuming that the latter results are representative of ion kinetic

(8) Jacobson, D. B.; Beauchamp, J. L.; Bowers, M. T., unpublished results.
(9) (a) Aristov, N.; Armentrout, P. B. *J. Am. Chem. Soc.* **1986**, *108*, 1806. (b) Elkind, J. L.; Ervin, K. N.; Aristov, N.; Armentrout, P. B., submitted for publication.
(10) Elkind, J. L.; Armentrout, P. B. *Inorg. Chem.* **1986**, *25*, 1078.
(11) Mandich, M. L.; Halle, L. F.; Beauchamp, J. L. *J. Am. Chem. Soc.* **1984**, *106*, 4403.
(12) Sallans, L.; Lane, K. R.; Squires, R. R.; Freiser, B. S. *J. Am. Chem. Soc.* **1985**, *107*, 4379.
(13) Tolbert, M. A.; Beauchamp, J. L. *J. Phys. Chem.*, submitted for publication.
(14) (a) Armentrout, P. B.; Beauchamp, J. L. *Chem. Phys.* **1980**, *50*, 21. (b) Armentrout, P. B.; Beauchamp, J. L. *J. Chem. Phys.* **1981**, *74*, 2819.
(15) Freas, R. B.; Ridge, D. P. *J. Am. Chem. Soc.* **1980**, *102*, 7129.
(16) Halle, L. F.; Armentrout, P. B.; Beauchamp, J. L. *J. Am. Chem. Soc.* **1981**, *103*, 962. For an interesting comparison of different ground-state and excited-state reactivities, see: Elkind, J. L.; Armentrout, P. B. *J. Am. Chem. Soc.* **1986**, *108*, 2765.
(17) Kang, H.; Beauchamp, J. L. *J. Phys. Chem.* **1985**, *89*, 3364.

Table II. Product Distributions for the Reactions of Ru^+, Rh^+, and Pd^+ with Alkanes at a Relative Kinetic Energy of 0.5 eV[a]

alkane	neutral prod.	Ru^+	Rh^+ 0.5 eV	Rh^+ 2.0 eV	Rh^+ ICR[b]	Pd^+
CH_4		N.R.	N.R.	N.R.	N.R.	*c*
C_2H_6	H_2	1.0[a]	1.0[a]	1.0[a]	1.0	N.R.
	total[d]	10	19	1.0		
C_3H_8	H_2	0.90[a]	0.97[a]	0.20[a]	0.94	0.54[a]
	$2H_2$	0.10	0.03	0.67	0.06	
	CH_4			0.13		0.46[a]
	total	40	40	8.0		6.3
n-C_4H_{10}	H_2	0.20[a]	0.27[a]			0.38[a]
	$2H_2$	0.80[a]	0.73[a]	0.88[a]	1.0	
	CH_4					0.21[a]
	C_2H_6			0.12		0.41[a]
	total	38	48	25		29
i-C_4H_{10}	H_2	0.73[a]	0.91[a]	0.10[a]	0.43	1.0[a]
	$2H_2$	0.21[a]	0.06	0.49	0.48	
	CH_4	0.02	0.01	0.08	0.09	
	H_2, CH_4	0.02	0.02	0.30		
	C_2H_6	0.02		0.03		
	total	95	65	30		110
neo-C_5H_{12}	H_2	0.22[a]	0.32[a]	0.03[a]	0.15	
	$2H_2$	0.05[a]	0.10[a]	0.21[a]	0.29	
	$3H_2$			0.05	0.02	
	CH_4	0.15[a]	0.40[a]	0.14[a]	0.13	1.0[a]
	CH_4, H_2	0.58[a]	0.07[a]	0.34[a]	0.34	
	C_2H_6		0.06[a]	0.07[a]	0.05	
	C_2H_6, H_2		0.05	0.11	0.02	
	C_3H_8			0.05		
	total	99	40	29		53

[a] Reaction products which clearly exhibited energy dependent cross sections characteristic of exothermic processes. [b] Product distributions for the reactions of Rh^+ reported in earlier ICR study (ref 5). [c] Not studied. [d] Total reaction cross sections, reported in A^2.

energies which are much higher than thermal energies. Some reactions observed in the previous ICR study are not observed in the present ion beam experiment at 0.5 eV but are seen at 2.0 eV (Table II). As an example, the energy dependence of the reactions of Rh^+ with 2-methylpropane are shown in Figure 2. Although the previous study reports three exothermic products (Table II), our results indicate that only loss of H_2 is exothermic. The other pathways clearly exhibit a translational energy threshold for reaction. The presence of electronically excited ions in the ICR experiment could also contribute to these differences.

Another explanation of the deivation between the ion beam and ICR results may lie in the time scale difference of the two experiments. Inspection of the differences between the two data sets reveals that the major discrepancies involve multiple elimination reactions. Multiple eliminations may be somewhat more prevalent in the ICR due to the longer reaction times (ms) relative to the reaction times in the present ion beam experiments (μs). However, this is not expected to account for all of the observed differences. The higher pressures of the ion beam experiment also cannot account for the observed differences; product distributions did not vary with pressure in the range employed in the ion beam experiment.

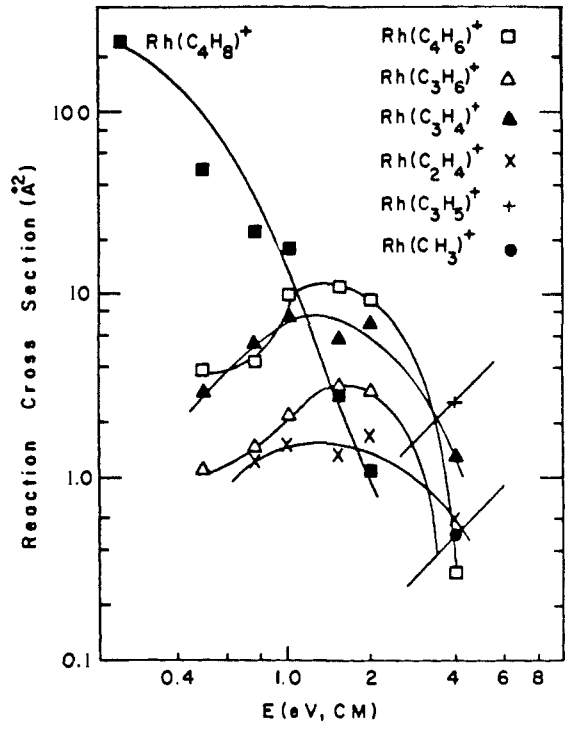

Figure 2. Variation in the experimental cross section for the reactions of Rh^+ with 2-methylpropane as a function of relative kinetic energy.

As indicated in Table II, the main exothermic reactions of Ru^+ and Rh^+ with small alkanes are observed to be single and double dehydrogenations. In contrast, the reaction of Pd^+ with alkanes leads to loss of smaller alkanes in addition to H_2. In order to gain insight into the specific reaction mechanisms, a study of the reactions of Ru^+, Rh^+, and Pd^+ with deuterium labeled alkanes was performed. The results for the exothermic dehydrogenation of labeled alkanes at low kinetic energy are given in Table III. The alkane loss products formed by using labeled alkanes are presented in Table IV.

In addition to reaction products such as those indicated in Tables II–IV, unreacted adduct ions are often observed in the ion beam

Table III. Isotopic Product Distributions for Dehydrogenation of Deuterated Alkanes by Ru^+, Rh^+, and Pd^+

		neutral product							
		single dehydrogenation			double dehydrogenation				
M^+	alkane	H_2	HD	D_2	$2H_2$	H_2 + HD	2HD or H_2 + D_2	D_2 + HD	$2D_2$
Ru^+	CH_3CD_3	0.15	0.73	0.12					
	$CH_3CD_2CH_3$	0.10	0.78	0.12[a]		0.58	0.42		
	$C(CH_3)_3D$	0.20	0.80			1.00			
	$CD_3CH_2CH_2CD_3$	0.20	0.46	0.34[b]	0.09[b]	0.30	0.38	0.17	0.06
Rh^+	CH_3CD_3	0.09	0.83	0.08					
	$CH_3CD_2CH_3$	0.14	0.79	0.07		0.71[c]	0.29[c]		
	$C(CH_3)_3D$	0.27	0.73			1.00			
	$CD_3CH_2CH_2CD_3$	0.32	0.61	0.07[a]	0.05	0.40	0.36	0.19	
Pd^+	$CH_3CD_2CH_3$		1.00						
	$C(CH_3)_3D$		1.00						
	$CD_3CH_2CH_2CD_3$	1.00							

[a] The identity of this product is uncertain due to the identical masses of D_2 and $2H_2$. To make the product distributions best match those in Table II, all of this mass product was assigned to be loss of D_2. [b] This product was assigned to be a 50:50 mixture of D_2 and $2H_2$ in order to make the product distributions best match those in Table II. [c] Product distribution at a relative kinetic energy of 1.0 eV.

Table IV. Isotopic Product Distributions for Alkane Loss from Deuterated Alkanes by Ru^+, Rh^+, and Pd^+ at a Relative Kinetic Energy of 1.0 eV

alkane	neutral prod.	Ru^+	Rh^+	Pd^+
$CH_3CD_2CH_3$	CH_4			1.0[a]
$C(CH_3)_3D$	CH_4	1.0	1.0	1.0
	$CH_4 + H_2$	0.5		
	$CH_4 + HD$	0.5	1.0	
$CD_3CH_2CH_2CD_3$	CD_3H			1.0[a]
	$C_2H_2D_4$			1.0[a]

[a] Product distribution at a relative kinetic energy of 0.5 eV.

Table V. Adduct Formation in the Reactions of Group 8–10 Metal Ions with Alkanes[a]

M^+	propane	isobutane	*n*-butane
Fe[b]	0.42	0.05	0.05
Co[b]	0.39	0.07	0.07
Ni[b]	0.25	0.09	0.06
Ru	0	0	0
Rh	0	0	0
Pd	0.35	0.23	0.57

[a] Fraction of the total product observed, normalized to 1.0, at a relative kinetic energy of 0.5 eV in the center-of-mass frame. The pressure of alkane gas was 1.5 mtorr. [b] Data from ref 39.

Table VI. Product Distributions for the Reactions of the Group 8–10 Transition-Metal Ions with Acetone at a Relative Kinetic Energy of 0.5 eV

neutral prod.	product distribution					
	Fe^+[a]	Co^+[a]	Ni^+[a]	Ru^+	Rh^+	Pd^+
CO	0.07	0.10	0.06	0.15	0.03	0.07
C_2H_6	0.93	0.90	0.94	0.19	0.27	0.93
CH_4				0.58	0.60	
$H_2 + CO$				0.08	0.10	

[a] Reference 18.

experiment at low relative kinetic energies. The extent of adduct formation for the first and second row group 8–10 metal ions reacting with alkanes is indicated in Table V. Although adduct ions are prevalent for Fe^+, Co^+, Ni^+, and Pd^+, no adducts are observed in the reactions of Ru^+ and Rh^+ with alkanes, even at elevated pressures.

In a related experiment aimed at obtaining thermochemical information, the exothermic reactions of Ru^+, Rh^+, and Pd^+ with acetone were studied. The exothermic products formed in these reactions are presented in Table VI. Also included in this table are previous ion beam results for Fe^+, Co^+, and Ni^+.[18] It can be seen that although the product distributions for Pd^+ closely resemble that of the first-row ions, two additional reactions, loss of CH_4 and loss of $(H_2 + CO)$,[19] are prevalent for Ru^+ and Rh^+. ICR studies reveal that methane loss was also the dominant process for Rh^+ reacting with acetone (91%).[20]

The fact that all three second-row metal ions lose CO in an exothermic process indicates that the sum of the first and second metal–methyl bond energies is greater than 96 kcal/mol.[21] Using previous values for the first metal–methyl bond energies (see Table I) implies $D(RuCH_3^+-CH_3) > 42$ kcal/mol, $D(RhCH_3^+-CH_3) > 49$ kcal/mol, and $D(PdCH_3^+-CH_3) > 37$ kcal/mol. Observation of exothermic loss of $(H_2 + CO)$ indicates that $D(M-C_2H_4^+) > 38$ kcal/mol for Ru^+ and Rh^+.[22] The lower limits to the bond dissociation energies obtained here will be used to estimate the energies of reaction intermediates discussed later in the paper.

Table VII. Exothermic Reactions of Rh–(Olefin)$^+$ Complexes with Small Molecules at a Relative Kinetic Energy of ≤0.25 eV

olefin	reactant	hydrogen loss			ethane loss		
		D_2	HD	H_2	C_2D_5H	$C_2D_4H_2$	$C_2H_4D_2$
$Rh-C_2H_4^+$	D_2		N.R.				
	CD_4		N.R.				
	C_2D_6	0.41[a]	0.46	0.13	0.50[b]	0.37[b]	0.13[b]
$Rh-C_3H_6^+$	D_2		1.0				
	CH_4		N.R.				
	C_2D_6	0.49[c]	0.33	0.18	0.64	0.26	0.10

[a] The product of this mass, $(C_2D_4)-Rh-(C_2H_4)^+$, could result from the reaction of $RhC_2D_4^+$ with C_2H_6 or from the reaction of $RhC_2H_4^+$ with C_2D_6. Because the primary dehydrogenation peaks are of equal intensity, this product was assigned to be a 50:50 mixture of the two processes. [b] Three exchange peaks were observed between $RhC_2H_4^+$ (mass = 136) and $RhC_2D_4^+$ (mass = 140). The double exchange peak (m = 138) was assigned to be a 50:50 mixture of exchange from ech of the primary dehydrogenation products. The mass 137 peak was assigned to be due primarily (75%) to single exchange from $RhC_2H_4^+$ and only 25% due to triple exchange from $RhC_2D_4^+$. The corresponding assignment was used for the mass 139 peak. [c] The product of this mass, $(C_2D_4)-Rh-(C_3H_6)^+$, could result from the reaction of either primary olefin. Because the ratio of primary dehydrogenation products favors formation of $RhC_3H_6^+$ by a factor of 3, this secondary reaction product was assigned to be primarily (75%) due to the reaction of $RhC_3H_6^+$ with C_2D_6.

Table VIII. Comparison of the Reactions of Group 8–10 Transition-Metal Ions with *n*-Butane at a Relative Kinetic Energy of 0.5 eV

neutral prod.	product distribution					
	Fe^+[a]	Co^+[a]	Ni^+[a]	Ru^+	Rh^+	Pd^+
H_2	0.20	0.29	0.48	0.20	0.27	0.38
$2H_2$				0.80	0.73	
CH_4	0.41	0.12	0.06			0.21
C_2H_6	0.39	0.59	0.45			0.41

[a] Reference 1c.

In a somewhat different experiment, sequential reactions of Rh^+ in multiple collisions were studied by using different combinations of reactant gases. The goal of these experiments was to determine the reactivity of Rh–(olefin)$^+$ complexes. For example, can Rh–(olefin)$^+$ complexes effect oxidative addition processes similar to those observed for bare rhodium ions? In an attempt to answer this question, the reactions of Rh^+ with a combination of ethane or propane and a reactant gas were studied. The results are indicated in Table VII. It can be seen that although D_2 and CD_4 do not react with $Rh(C_2H_4)^+$, C_2D_6 reacts to lose H_2, HD, and D_2 as exothermic processes. This reaction was also observed with unlabeled ethane in a previous ICR study.[5] The implications of observing this reaction to be exothermic will be discussed later.

In certain cases, the products of the multiple collision reactions could result from two possible reaction sequences. For example, in the reaction of Rh^+ with C_2H_6 and C_2D_6, the product $(C_2H_4)-Rh-(C_2D_4)^+$ could be formed from either $Rh-(C_2H_4)^+$ reacting with C_2D_6 or $Rh-(C_2D_4)^+$ reacting with C_2H_6. In this case, because the primary dehydrogenation products were equally abundant, half of the product in question was estimated to result from each source. There were similar ambiguities in the reactions of Rh^+ with C_3H_8 and C_2D_6 simultaneously. The products were assigned based on the relative intensity of the primary olefin products. The secondary reactions presented in Table V do *not* occur for Fe^+, Co^+, or Ni^+.[23] This important difference between

(18) Halle, L. F.; Crowe, W. E.; Armentrout, P. B.; Beauchamp, J. L. *Organometallics* **1984**, *3*, 1694.

(19) Loss of $(H_2 + CO)$ cannot be distinguished from loss of H_2CO in this experiment. Formation of the former product is the favored process by 0.5 kcal/mol (ref 21).

(20) Bryd, G. D., PhD Thesis, Purdue University, 1982, p 134.

(21) Auxiliary heats of formation are taken from Cox, J. D.; Pilcher, G. *Thermochemistry of Organic and Organometallic Compounds*; Academic Press: New York, 1970. $\Delta H_f(CH_3) = 35.1$ kcal/mol from McMillen, D. F.; Golden, D. M. *Ann. Rev. Phys. Chem.* **1982**, *33*, 493.

(22) Another possible structure for this product is $CH_2RhCH_2^+$. If this were the product formed, then the reaction exothermicity implies $D(Rh^+-2CH_2) > 210$ kcal/mol. The $RhCH_2^+$ bond strength has been determined previously to be 94 ± 5 kcal/mol (Jacobson, D. B.; Freiser, B. S. *J. Am. Chem. Soc.*, in press). It therefore seems unlikely that the biscarbene ion is being formed in the reaction with acetone.

Scheme I

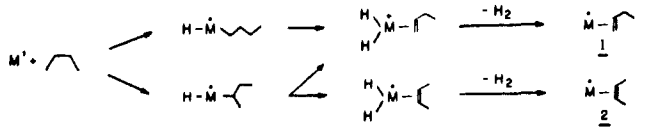

the first- and second-row transition-metal ions gives information about the potential energy surfaces which govern the reactions of atomic transition-metal ions with saturated hydrocarbons.

Discussion

The reactions of Ru^+ and Rh^+ with alkanes are fairly similar and are dominated by the loss of one or more molecules of H_2. A comparison of the products formed in the reaction of *n*-butane with the first and second row group 8–10 metal ions is given in Table VIII. It is seen that the reactivity of Ru^+ and Rh^+ does not resemble that of their first-row congeners, Fe^+ and Co^+. Several questions arise regarding this differential reactivity. First, why does multiple loss of hydrogen occur for Ru^+ and Rh^+? Second, why are alkane loss channels not prevalent with Ru^+ and Rh^+? Finally, although all of the metal ions exothermically dehydrogenate alkanes, is the dehydrogenation mechanism the same in all cases? These questions will be addressed below.

In contrast to Ru^+ and Rh^+, the reactivity of Pd^+ appears at first glance to be remarkably similar to the first-row metal ions Fe^+, Co^+, and Ni^+ (see Tables VI and VIII). However, the uniquely high Lewis acidity of Pd^+ results in distinctive reactivity as discussed below.

Dehydrogenation Mechanism for Ru^+ and Rh^+. Remarkable metal specificity has recently been observed in the dehydrogenation reactions of alkanes by transition-metal ions in the gas phase. Studies of product ion structures[2b,3b,7,15,24] in conjunction with experiments involving deuterium labeled *n*-butane-*1,1,1,4,4,4-d*$_6$[1c,4,25] reveal at least three distinct mechanisms. Sc^+ has been shown to undergo a 1,3-dehydrogenation,[4] whereas Co^+ and Ni^+ effect 1,4-dehydrogenations forming bisolefin complexes.[3b,7] Dehydrogenation at Fe^+ centers appears to occur via a combination of 1,2- and 1,4-mechanisms.[3b,8] These latter two mechanisms are illustrated in Schemes I and II.

The product distributions observed for the reactions of Ru^+ and Rh^+ with small labeled alkanes (Table VIII) indicates a predominantly 1,2-dehydrogenation mechanism.[26] For example, the main product observed with 2-methylpropane-*2-d*$_1$ is loss of HD. Scrambling leads to the loss of a smaller amount of H_2, a process not observed for the first-row metal ions. The presence of scrambled products is consistent with low barriers for β-H transfer for Ru^+ and Rh^+. This will be discussed in more detail later. It is also possible that the scrambled products are actually the result of 1,1-elimination. These two processes cannot be distinguished in this experiment.

The results of the dehydrogenation of *n*-butane by Ru^+ and Rh^+ are also *consistent* with a 1,2-mechanism. Arguments presented below against a 1,4-mechanism indirectly support this assignment. The 1,4-mechanism depicted in Scheme II involves either initial C–C bond insertion or C–H bond insertion followed by β-ethyl transfer. As will be discussed later, there is evidence that neither exothermic C–C bond insertions or competitive β-alkyl transfers occur at Ru^+ and Rh^+ centers. Furthermore, any elimination mechanisms proposed must accommodate the loss of a *second* H_2 molecule from *n*-butane, as indicated in Table II. A 1,2-dehydrogenation mechanism leaves the metal–olefin complex in a geometry favorable for elimination of a second H_2 molecule via allylic hydrogen transfers from **1** or **2** as indicated in Scheme III. However, the product of the 1,4-elimination, a bisolefin complex

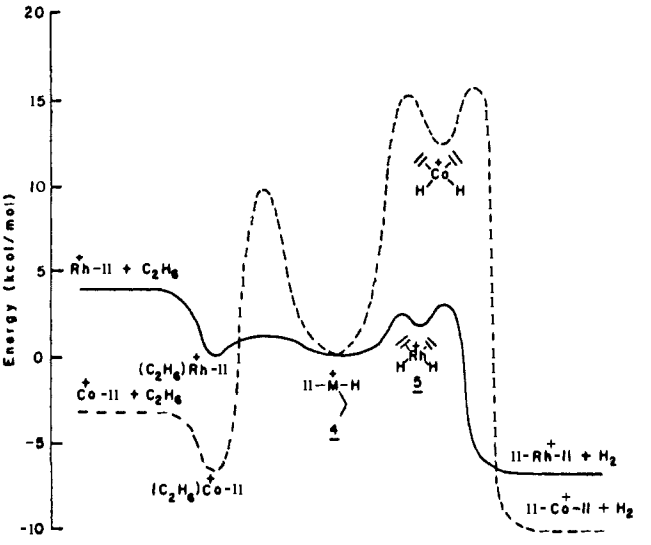

Figure 3. Qualitative potential energy diagram for the decomposition of $(C_2H_4)MH(C_2H_5)^+$ for M = Rh and Co. The products corresponding to loss of ethane are shown on the left, and those corresponding to loss of H_2 are shown on the right. The bond energies used for calculating the energies of the Co^+ intermediates are given in ref 7. The bond energies to Rh^+ were estimated to be $D(Rh^+–C_2H_4)$ = 43, $D(Rh^+–2C_2H_4)$ = 102, $D[(C_2H_4)_2RhH^+–H]$ + $D[(C_2H_4)_2Rh^+–H]$ = 95, and $D[(C_2H_4)RhH^+–R]$ + $D[(C_2H_4)Rh^+–H]$ = 102 kcal/mol. These bond energies are consistent with the bond energies given in Table I and the lower limits discussed in the Results section.

3, may not easily rearrange to eliminate a second molecule of H_2. In ICR experiments, reaction 3 has been observed to occur very

$$Rh(C_2H_4)^+ + C_2H_4 \rightarrow Rh(C_4H_6)^+ + H_2 \qquad (3)$$

slowly, with a rate of less than 1% of the calculated encounter rate.[27] Because the $Rh(C_2H_4)_2^+$ adduct formed in reaction 3 has *at least* 12 kcal/mol more internal energy than would **3** formed by reaction with *n*-butane, it is unlikely that **3** would be able to react to lose H_2 to any significant extent. This evidence against a 1,4-mechanism lends support to the proposed 1,2-dehydrogenation mechanism for Ru^+ and Rh^+.

Observation of Multiple Hydrogen Loss in the Reactions of Ru^+ and Rh^+. As indicated in Table VIII, Ru^+ and Rh^+ react with *n*-butane to lose two molecules of H_2, a process that is not observed for the first-row transition-metal ions as an exothermic reaction. The differences in observed reactivity reflect differences in the potential energy surfaces that connect the reactants to the products. Recently, kinetic energy release distributions have been measured for metastable decompositions of Fe^+, Co^+, and Ni^+ adducts with *n*-butane.[7,8] High translational energy releases were observed for the dehydrogenation reactions, indicating the existence of large activation barriers for the reverse association reactions. The barrier for reductive elimination of alkanes from Co–(olefin)$^+$ intermediates is not known. However, it has been suggested that there might be a substantial barrier for this process as well.[7] A simplified potential energy surface indicating these proposed barriers is illustrated in Figure 3, where intermediate **4** can competitively decompose to lose H_2 or C_2H_6. Based on the above observations, reaction 4 should have a significant activation barrier for Fe^+,

$$M(C_2H_4)^+ + C_2H_6 \rightarrow M(C_2H_4)_2^+ + H_2 \qquad (4)$$

Co^+ and Ni^+. This is supported by the fact that reaction 4 has *not* been observed for any of the first row group 8–10 metal ions.[23]

The activation parameters which govern the reactions of Rh^+ must be quite different than those observed for Fe^+, Co^+ and Ni^+. As indicated in Table VII, reaction 4 is observed to be an exothermic process for Rh^+. Therefore, this process must occur *without* a large activation barrier for Rh^+. In fact, there can be

(23) Jacobson, D. B.; Freiser, B. S. *J. Am. Chem. Soc.*, in press.
(24) Jacobson, D. B.; Freiser, B. S. *J. Am. Chem. Soc.* **1983**, *105*, 736.
(25) Halle, L. F.; Houriet, R.; Kappes, M. M.; Staley, R. H.; Beauchamp, J. L. *J. Am. Chem. Soc.* **1982**, *104*, 6293.
(26) The term 1,2-elimination implies that the hydrogen atoms are eliminated from adjacent carbon atoms. This term does not specify which carbon atoms are involved in the elimination.
(27) This reaction is reported in Jacobson, D. B.; Freiser, B. S. *J. Am. Chem. Soc.*, in press. The rate of this reaction was obtained from Jacobson, D. B., private communication.

Scheme II

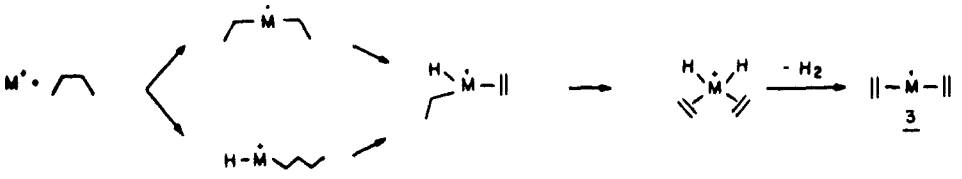

Scheme III

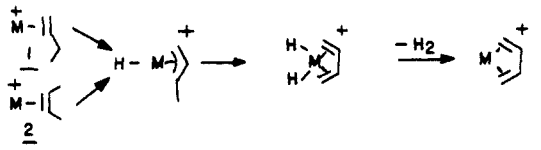

essentially no barrier for oxidative addition of R–H at $Rh(C_2H_4)^+$ centers and a barrier of less than 4 kcal/mol for either β-H transfer from intermediate **4** or reductive-elimination of H_2 from intermediate **5**, as indicated in Figure 3. The abundance of scrambled products in reaction 4 using labeled C_2D_6 indicates that the barrier for insertion of the olefin into the metal hydrogen bond in **5** is lower than the barrier for H_2 elimination or that the frequency factor is higher. In other words, the β-hydrogen transfer process which connects **4** to **5** can occur reversibly several times prior to elimination of H_2 from **5**. This is indicated in Figure 3.

Other evidence that the reaction barriers in the potential energy surfaces of the first- and second-row transition-metal ions are vastly different can be obtained from an analysis of the degree to which long-lived adduct ions are formed. As indicated in Table V, although adduct ions are prevalent for Fe^+, Co^+, Ni^+, and Pd^+, they are not observed for Ru^+ and Rh^+, even at elevated pressures. An example of an adduct formation reaction in the ion beam experiment is indicated in Scheme IV for the case of a metal ion reacting with propane. The adduct ion detected can have any of a number of different structures. One possible structure is the initially formed collision complex, **6**, held together by ion-induced dipole interactions. The adduct ion could also be an inserted species such as **7** or a rearranged complex as indicated by **8**. Since only the mass of the adduct ion is detected in this experiment, differentiation of these structures is not possible.

The overall rate of adduct decomposition depends on the rates for the various reaction steps in Scheme IV. The relative activation parameters for C–H bond insertion, β-hydrogen transfer, and H_2 elimination determine which adduct structure is dominant. At low pressures, if the overall decomposition rate is slow enough ($<4 \times 10^4\ s^{-1}$), then the internally excited adducts will be detected directly. The products which are detected under these conditions include species which might be stabilized by emission of an infrared photon on a longer time scale. At high pressures, if the adduct decomposition rate is slow enough ($<10^6\ s^{-1}$), the adducts may live long enough to suffer a second stabilizing collision. In this case, sufficiently cooled adducts will be detected. For overall reaction rates $>10^7\ s^{-1}$, it is unlikely that any adduct would be detected, even at elevated pressures. The fact that no adducts are observed for Ru^+ and Rh^+ thus indicates faster rearrangement and dissociation rates of the various reaction intermediates in comparison to their first-row congeners. This is consistent with the very small β-H transfer and reductive elimination barriers proposed above for Ru^+ and Rh^+.

The implications of low H_2 elimination barriers for the potential energy surfaces of Ru^+ and Rh^+ reactions can be seen in the dehydrogenation reaction of *n*-butane. As discussed above, Ru^+ and Rh^+ appear to dehydrogenate *n*-butane by a 1,2-elimination mechanism. As discussed in ref 7, if no energy redistribution occurs after the transition state for dehydrogenation ("late barrier"), then the entire reverse activation barrier will appear as product translation. The remainder of the available energy will be partitioned statistically between the reaction coordinate and all other internal degrees of freedom.

In accord with the low barrier for reductive elimination of H_2 from **5** (Figure 3), the elimination of H_2 to form **1** or **2** (Scheme I) is expected to proceed without a large barrier. Therefore, it is expected that the dehydrogenation products will be formed with relatively low translational energy and thus relatively high internal energy. The high internal excitation of $Rh(C_4H_8)^+$ may result in the occurrence of a subsequent reaction, i.e., loss of a second molecule of H_2.

Absence of Alkane Loss Products for Ru^+ and Rh^+. As indicated in Figure 2, the only clearly exothermic product observed in the reaction of Rh^+ with 2-methylpropane is H_2 loss. Although loss of CH_4 is the thermochemically preferred product,[28] it is *not* observed at low energy and becomes prominent only at relative kinetic energies in the range 1–2 ev. Two mechanisms have been proposed previously for the loss of CH_4 from 2-methylpropane in the reaction of Fe^+, Co^+, and Ni^+.[1b] One involves insertion of the metal ion into a C–C bond, followed by β-H transfer and subsequent reductive elimination of CH_4. Alternatively, insertion into a C–H bond can be followed by β-methyl transfer and elimination of CH_4. The lack of alkane loss processes for Ru^+ and Rh^+ indicates that *neither* of the above processes occurs for these metal ions.

This difference in reactivity between the first- and second-row metal ions may be attributed to differences in any of three steps: (1) initial insertion into a C–C vs. C–H bond (2) β-H transfer vs. β-alkyl transfer, and (3) reductive elimination of HR vs. reversible β-H transfers. As discussed previously, the barrier for reductive elimination of HR from Rh–(olefin)$^+$ complexes is very small. Therefore, it is unlikely that the lack of alkane loss observed for Ru^+ and Rh^+ is a result of noncompetitive HR elimination. Furthermore, β-hydrogen transfers are thought to be facile for Rh^+ (Figure 3). Accordingly, an activation barrier or an extremely low frequency factor for carbon–carbon bond insertion by Ru^+ and Rh^+ is postulated. Hydrogen loss products are observed in abundance for Ru^+ and Rh^+ reacting with alkanes. The first step in these processes is most certainly exothermic C–H bond insertion. Therefore, the activation barrier for β-methyl transfer must be much higher than for β-hydrogen transfer or the frequency factor much lower. This renders β-methyl transfer unable to compete with β-hydrogen transfer and results in the observation of only H_2 loss products.

An important exception is the loss of CH_4 observed in the reaction of 2,2-dimethylpropane with Ru^+ and Rh^+. In fact, loss of CH_4 is the major exothermic reaction observed at low energy for Rh^+. This is consistent with the above ideas in that, after C–H insertion, no β-H's are available, which then permits competitive transfers of less favorable groups such as CH_3. Furthermore, once β-methyl transfer occurs to form a hydridoalkyl–rhodium complex, there is essentially no barrier for elimination of RH. Thus the Rh–(olefin)$^+$ complex is formed with very high internal excitation which allows the products to react further. This is consistent with the prevalent loss of $(CH_4 + H_2)$ in the reactions of Ru^+ and Rh^+ with 2,2-dimethylpropane at low energies and with 2-methylpropane at higher energies. In these reactions, it is also possible that the H_2 molecule is lost first, followed by elimination of methane from the highly excited metal–olefin complex. Studies with deuterium labeled 2-methylpropane-*2*-d_1 (Table IV) indicate that the methane lost in the reactions with Ru^+ and Rh^+ is purely CH_4. Furthermore, although a 50:50 mixture of $(CH_4 + H_2)$ and CH_4 + HD) loss is observed in the reaction with Ru^+, only the latter product is observed for Rh^+. From these data alone, it is not possible to explain this difference in the reactivity between

(28) If the bond strengths of propylene and isobutene to Rh^+ are assumed to be equal, then loss of methane is thermochemically favored over H_2 loss by 9 kcal/mol; see ref 21.

Scheme IV

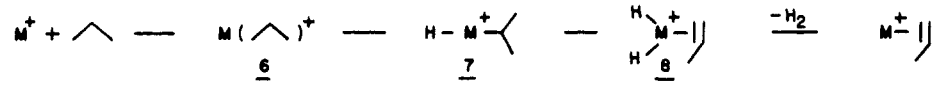

Ru^+ and Rh^+ or to predict which molecule is eliminated first in this multiple loss process. Collisional stabilization studies or metastable decompositions could give information about the sequence in which the products are formed.

The reactions of Ru^+ and Rh^+ with acetone are also consistent with the idea that C–H bond insertions are favored over C–C insertions. After initial C–H bond insertion, the lack of β-H's results in the transfer of a β-methyl group and elimination of CH_4. Although this is by far the dominant process for Ru^+ and Rh^+, it is not observed in the ion beam experiment with Fe^+, Co^+, or Ni^+ (Table VI).

Comparison of First- and Second-Row Transition-Metal Ion Reactivity. The difference in reactivity between Ru^+ and Rh^+ and their first-row congeners suggests differences in the potential energy surfaces which are summarized below. First, whereas Fe^+, Co^+, and Ni^+ complexes have large activation barriers for reductive elimination of H_2 and possibly HR, the corresponding eliminations at Ru^+ and Rh^+ centers appear to have little or no barriers. Second, there may be differences in the activation parameters for carbon–carbon bond insertion by transition-metal ions of the first and second row. Although C–C bond activation has been proposed for reactions occurring at Fe^+, Co^+, and Ni^+ centers,[1c,3b,25] in most cases the results may also be explained by C–H bond insertion followed by β-alkyl shifts. Unfortunately, labeling studies do not differentiate these two mechanisms. In contrast, results for the second-row metal ions clearly indicate that Ru^+ and Rh^+ do not exothermically cleave C–C bonds. Finally, there may be differences in the relative activation parameters for β-H and β-alkyl transfers for the first- and second-row metal ions. Although there are few unequivocal observations of β-methyl transfers for gas-phase transition-metal ions, there is evidence for competitive β-methyl transfers at Fe^+ centers.[1c] Migratory insertions of ethylene into the $M-CH_3^+$ bond of Co^+,[29] Sc^+,[4] and Ti^+ [30] complexes also indicate that β-methyl transfers can occur for the first-row transition-metal ions. Similar β-methyl transfers do *not* occur in competition with β-hydrogen transfers for Ru^+ and Rh^+.

It is possible that the observed differences in the activation parameters for the processes discussed above may be related to bonding differences for the first-row vs. second-row transition-metal ions. Clues into these differences can be obtained from an examination of the bond strengths and bonding orbitals used for the transition-metal ion reactions.

Ab initio calculations on the ground states of the diatomic metal hydrides FeH^+, CoH^+, and NiH^+ indicate that the bonding in these molecules involves a metal orbital which is 85–90% s-like in character.[31] This is in agreement with the experimentally observed trend that the M^+-H bond dissociation energies for the first-row transition metals increase with decreasing promotion energy from the ground state to a state with an electronic configuration which is s^1d^n, indicating a bond that involves a metal 4s orbital.[32] Because the first bond utilizes what is primarily a 4s orbital, formation of a *second* bond to Fe^+, Co^+, and Ni^+ involves primarily a metal 3d orbital.[31] The second bond is thus inherently weaker than the first due to the smaller size and poorer overlap of the 3d orbital relative to the 4s orbital. For example, the strength of the *second* bond in dimethylcobalt ion, $D(CoCH_3^+-CH_3)$ = 45 kcal/mol,[7b] is considerably less than the strength of the first bond, $D(Co^+-CH_3)$ = 61 kcal/mol. This is the case even though formation of the first bond requires promotion of Co^+ to an s^1d^n configuration, as discussed above for CoH^+.

The description of the bonding to the second-row metal ions, however, is quite different. When bonding a hydrogen atom to the ground states of Ru^+, Rh^+, and Pd^+, which are all derived from d^n configurations, the metal orbital involved is predominantly d-like in character.[11] This is due to the more similar size of the 5s and 4d orbitals in the second-row transition series. Thus, the *second* bond to Ru^+-H and $Rh-H^+$ might be expected to have the *same* inherent bond energy as the first bond. Furthermore, because less exchange energy is lost in forming the second bond to a d-orbital, the second bond might actually be stronger than the first.[33] However, as indicated in Table I, the first bond energy tends to be somewhat greater for the first-row metal ions than for the second row.[34] Therefore, the sum of the first and second bond energies may be comparable for the metal ions of both rows. It is thus unlikely that the observed differences in reactivity are a direct result of the strengths of the bonds in the transition-metal reaction intermediates. Note, however, that the orbitals used in forming these bonds are quite different for the metal ions of the two rows, and this may be responsible for the differential reactivity.

The s–d hybrid orbitals used in the first-row bonding are much more diffuse than the pure d orbitals used for the second-row bonds.[35] The second-row 4d orbitals are also much smaller than the first-row 4s orbitals.[35] This difference is reflected in the shorter bond lengths for RuH^+ and RhH^+ relative to FeH^+ and CoH^+.[35] When inserting into a very directional C–C bond, more favorable overlap may be possible by using relatively large, diffuse s–d hybrid orbitals than when using two tight d orbitals. It has been recently pointed out that metal d-orbital character is essential for facile β-H transfers involving a four center transition state.[36] However, due to the directionality of a methyl orbital, less bonding is expected in the transition state for β-methyl transfer than for β-H transfer. This may be more of a problem for the second-row transition-metal ions where tight metal d orbitals are involved. Perhaps more diffuse s–d hybrid orbitals provide better overlap in the transition state for β-methyl transfer. It is thus possible that the d^n configurations of the second-row transition-metal ions favor insertion into less directional bonds, i.e., the C–H bonds of alkanes, and also favor transfer of a spherically symmetric hydrogen atom.

The orbitals used for bonding may also be useful in understanding the relatively low barriers for reductive elimination of H_2 in the reactions of the second-row vs. first-row transition-metal ions. Recent calculations indicate that the bond angle of MH_2^+ can be much smaller for bonds that have a significant amount of d-orbital character. For example, the hydrogen bonds to Mo^+ in MoH_2^+ are 80% *d* in character with a bond angle of 64°.[37] In contrast, the hydrogen bonds to Sc^+ in ScH_2^+ are only 50% *d* with a bond angle of 106°.[38] If this trend is true in general, then

(29) Jacobson, D. B.; Freiser, B. S. *J. Am. Chem. Soc.*, in press.
(30) Uppal, J. S.; Johnson, D. E.; Staley, R. H. *J. Am. Chem. Soc.* **1981**, *103*, 508.
(31) Schilling, J. B.; Goddard, W. A., III.; Beauchamp, J. L. *J. Am. Chem. Soc.* **1986**, *108*, 582. The major contribution to the bonding in first-row metal hydrides typically comes from the s and d orbitals, with less than 10% p character. More recent calculations for metal hydrides indicate similar results, with only minor involvement of the p orbitals in bonding (Schilling, J. B., unpublished results).
(32) Armentrout, P. B.; Halle, L. F.; Beauchamp, J. L. *J. Am. Chem. Soc.* **1981**, *103*, 6501.
(33) Formation of the first d-type bond in Ru^+ and Rh^+ requires uncoupling of the high spin metal configuration, which somewhat weakens the resulting bond. The second bond does not suffer this same energetic loss and is therefore expected, on this basis, to be somewhat stronger than the first. See ref 11 for further discussion.
(34) The inherent bond energies of H and CH_3 to the first-row transition-metal ions were shown to be 60 and 70 kcal/mol, respectively, ref 32. Although no such inherent bond energies have been determined for the second-row metal ions, the values presented in Table I are typically lower than for the first row.
(35) Schilling, J. B.; Goddard, W. A., III.; Beauchamp, J. L., to be submitted to *J Am. Chem. Soc.*
(36) Steigerwald, M. L.; Goddard, W. A., III. *J. Am. Chem. Soc.* **1984**, *106*, 308.
(37) Calculations indicate that the lowest energy configuration for this molecule is not an η^2 complex, but rather consists of two σ M–H bonds (Schilling, J. B.; Goddard, W. A., III.; Beauchamp, J. L., work in progress).
(38) Alvarado-Swaisgood, A. E.; Harrison, J. F., submitted for publication.

smaller bond angles for the second-row metal ions may result in lower activation barriers for reductive elimination of H_2 relative to the first row.

Reaction Mechanism for Alkane Activation by Pd^+. The product distributions for the reactions of Pd^+ with alkanes are seemingly quite similar to those observed for Fe^+, Co^+, and Ni^+ as indicated in Tables VI and VIII. In fact, the alkane loss products resulting from the reactions of Pd^+ with deuterium labeled alkanes (Table IV) are almost identical with those observed for Fe^+, Co^+, and Ni^+.[1c] However, closer inspection of the hydrogen loss products reveals some substantial differences in reactivity. For example, reaction of Pd^+ with *n*-butane-*1,1,1,4,4,4-d*$_6$ yields exclusive elimination of H_2, in contrast to the scrambled products observed for Fe^+ and Co^+ and loss of D_2 for Ni^+.[1c,2b,3b] Both Co^+ and Ni^+ dehydrogenate *n*-butane exclusively via a 1,4-mechanism, with scrambling occurring in the Co^+ case.[7] In contrast, dehydrogenation by Pd^+ appears to occur by a quite distinct 1,2-mechanism across the central C–C bond exclusively.

Another difference in the reactivity of Pd^+ can be found from an examination of the overall reaction cross sections. Palladium ions react with branched alkanes to a much larger extent that with linear alkanes. Although this trend also occurs for Ru^+ and Rh^+, it is much less pronounced. The opposite trend occurs for Fe^+, Co^+, and Ni^+.[39]

An examination of the bonding to Pd^+ gives insight into its unusual reactivity. The configuration giving rise to the ^2D ground state of Pd^+ is $4d^9$,[40] which has only one unpaired electron available for formation of a covalent bond. In this respect, Pd^+ is quite similar to its first-row congener Ni^+ ($3d^9$). The high reactivity of Ni^+ is thought to be a result of the low promotion energy (only 23 kcal/mol) required to excite Ni^+ to a bonding s^1d^8 configuration which is able to make up to three covalent bonds. In contrast, the promotion energy required to excite Pd^+ to a bonding s^1d^8 configuration is much larger, 83 kcal/mol. The high promotion energy of Cr^+ from the ground state (^6S derived from the d^5 configuration) to the lowest state (derived from a s^1d^4 configuration) has been invoked to explain the low reactivity of this species with hydrocarbons.[32] This raises the question of how Pd^+ is able to activate alkanes at all.

Possible mechanisms for the activation of alkanes by Pd^+ involve using different oxidation states of palladium. For example, Pd^+ may insert into alkane C–H or C–C bonds by H^- or R^- abstraction, leading to Pd(0) complexes as shown in structures **9** and **10**, respectively. In these structures, the alkyl cation remains bound to the metal center by acid–base interactions.

$$\underset{\mathbf{9}}{H\text{–}Pd^0\text{–}R^+} \qquad \underset{\mathbf{10}}{R_1\text{–}Pd^0\text{–}R_2^+ \leftrightarrow R_1^+\text{–}Pd^0\text{–}R_2}$$

The configuration giving rise to the ^1S ground state of Pd(0) is $4d^{10}$, which is unable to make any covalent bonds. However, the promotion energy to the $5s^14d^9$ configuration favorable for bonding is only 18.7 kcal/mol.[40] The bonding in intermediates such as **9** would then involve a covalent bond to H using the singly occupied 5s orbital and a donor–acceptor bond to R^+ using a filled 4d orbital as illustrated schematically by **11** and **12**.

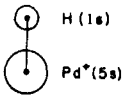

11

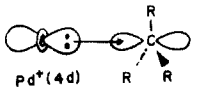

12

The hydride affinities for a number of transition-metal ions have been recently measured and are illustrated in Figure 4.[12,13,41] It is seen that the hydride affinity of Pd^+ is comparable to that of tertiary alkyl cations. Thus formation of intermediates such as

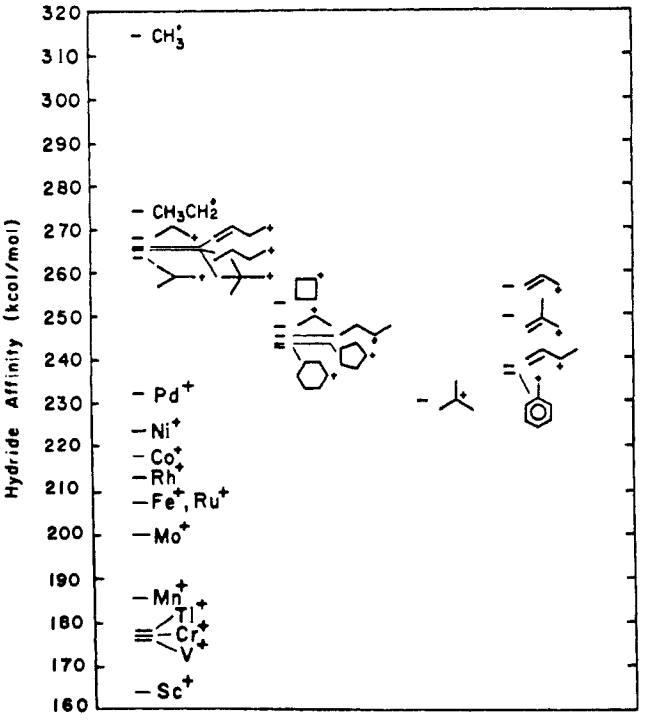

Figure 4. Hydride affinities for gas-phase metal ions and alkyl cations.

9 are energetically reasonable for tertiary C–H bond insertion and are possible for secondary C–H insertion if the strength of the donor–acceptor bond is greater than 16 kcal/mol. The hydride affinities of Cr^+ and Mn^+ are much lower,[42] making hydride abstraction energetically unreasonable as a first step in C–H bond activation by these ions.

As indicated in Figure 4, primary C–H insertion by Pd^+ requires a donor–acceptor bond energy in excess of 35 kcal/mol. It is possible that this energy requirement renders primary hydride abstraction unreasonable. In this case, another mechanism must be invoked to explain the reaction of Pd^+ with 2,2-dimethylpropane to lose CH_4. Insertion into a C–C bond in this case would form an intermediate such as **10** where the charge is delocalized as shown by the two canonical forms, perhaps rendering C–C insertions by Pd^+ a favorable reaction pathway. Unfortunately, this cannot be quantified due to lack of thermochemical data. These ideas correctly predict that ethane should be unreactive toward Pd^+. No reaction is observed because after initial C–C insertion to form **10**, only thermodynamically unfavorable products could be formed, namely, CH_4 and $PdCH_2^+$ via α-hydrogen abstraction.[43]

The hydride abstraction model presented above is supported by the reaction of Pd^+ with deuterium labeled *n*-butane-*1,1,1,4,4,4-d*$_6$. The only dehydrogenation product observed in this reaction is loss of H_2. A 1,2-mechanism across the central C–C bond would be expected for a reaction which proceeds via a carbonium ion intermediate. For example, the gas phase ionic dehydration of 2-butanol via a carbonium ion intermediate occurs to produce predominantly 2-butene as opposed to 1-butene.[44] Dehydration of 2-butanol on Al_2O_3 surfaces also produces mainly 2-butene.[45] This supports our belief that we are indeed observing hydride abstraction as a first step in the reactions of Pd^+ with

(39) Halle, L. F.; Armentrout, P. B.; Beauchamp, J. L., unpublished results.

(40) Moore, C. E. *Atomic Energy Levels*, National Bureau of Standards: Washington, D. C., 1949.

(41) The hydride affinities for the cationic alkyl species in Figure 5 are from the following: Schultz, J. C.; Houle, F. A.; Beauchamp, J. L. *J. Am. Chem. Soc.* **1984**, *106*, 7336.

(42) The homolytic Mn–H bond dissociation energy is not well-known. The experimental values are contradictory and range from 56 to <32 kcal/mol. This problem is discussed in Squires, R. R. *J. Am. Chem. Soc.* **1985**, *107*, 4385. A value of D(Mn–H) = 32 kcal/mol was used for Figure 5. The Mn^+ hydride affinity is equal to D(Mn–H) + IP(Mn) – EA(H), where IP(Mn) = 7.43 ev (ref 40), and EA(H) = 17.4 kcal/mol.

(43) Typical M^+–CH_2 bond strengths are 70–90 kcal/mol (ref 32). Using this range, $Pd^+ + C_2H_6 \rightarrow PdCH_2^+ CH_4$ is expected to be endothermic by 4–24 kcal/mol. Activation barriers for α-H transfer may make this an even less favorable process.

(44) Beauchamp, J. L.; Caserio, M. C. *J. Am. Chem. Soc.* **1972**, *94*, 2638.

(45) Pines. H.; Haag, W. O. *J. Am. Chem. Soc.* **1961**, *83*, 2047.

saturated alkanes. It should be noted that in condensed phase studies at Pd(II) centers, carbonium ion intermediates have been previously proposed.[46] For example, oligomerization and isomerization of olefins by $Pd(CH_3CN)_4^{2+}$ have been proposed to proceed via carbonium ion intermediates.

Conclusion

The reactivities of Ru^+, Rh^+, and Pd^+ are shown to be remarkably different from their first-row congeners. Whereas Co^+ and Ni^+ dehydrogenate alkanes by a 1,4-elimination mechanism, the corresponding second-row metal ions appear to effect 1,2-dehydrogenations. The reactions of Ru^+ and Rh^+ are characterized by C-H insertions and facile β-H transfers. Unlike their first-row congeners, β-methyl transfers, and C-C insertions do not occur for Ru^+ and Rh^+. Furthermore, the barriers for reductive elimination of RH and H_2 from Rh-(olefin)$^+$ complexes are quite small, in contrast to those proposed previously for Co^+. This may result in high internal excitation of the primary dehydrogenation products for Ru^+ and Rh^+ reactions. In this case, the products themselves may undergo an exothermic elimination of a second molecule of H_2, a process not observed for the first row group 8-10 metals ions. These differences in reactivity are proposed to be due to differences in the sizes and shapes of the bonding orbitals for the first- and second-row metal ions.

The mechanism by which alkanes are activated by Pd^+ is quite distinct from any other metal ion studied to date. It is proposed that the uniquely high Lewis acidity of Pd^+ results in a hydride abstraction mechanism for C-H bond activation.

Acknowledgment. This work was supported by the National Science Foundation under Grant CHE-8407857. M.I.M. is grateful to the Bantrell Foundation for a postdoctoral fellowship.

Registry No. Ru^+, 20019-76-5; Rh^+, 20561-59-5; Pd^+, 20561-55-1; CH_4, 74-82-8; C_2H_6, 74-84-0; C_3H_8, 74-98-6; n-C_4H_{10}, 106-97-8; i-C_4H_{10}, 75-28-5; neo-C_5H_{12}, 463-82-1; $RhC_2H_4^+$, 103639-31-2; $RhC_3H_6^+$, 103639-32-3.

(46) Sen, A.; Lai, T. W. *J. Am. Chem. Soc.* **1981**, *103*, 4627.

Gas-Phase Hydration Reactions of Protonated Alcohols. Energetics and Bulk Hydration of Cluster Ions

K. Hiraoka,* H. Takimoto, and K. Morise

Contribution from the Faculty of Engineering, Yamanashi University, Takeda-4, Kofu 400, Japan. *Received December 10, 1985*

Abstract: The gas-phase equilibria for hydration reactions of protonated methyl alcohol, ethyl alcohol, n-propyl alcohol, and isopropyl alcohol, $ROH_2^+(H_2O)_{n-1} + H_2O = ROH_2^+(H_2O)_n$, were measured with a pulsed electron beam mass spectrometer. van't Hoff plots of the equilibrium constants lead to $\Delta H°_{n-1,n}$ and $\Delta S°_{n-1,n}$ up to $n = 6$. While the proton affinities increase in the order methyl alcohol < ethyl alcohol < n-propyl alcohol < isopropyl alcohol, the stabilities of clusters $ROH_2^+(H_2O)_n$ toward dissociation increase in the reverse order, i.e., isopropyl alcohol < n-propyl alcohol < ethyl alcohol < methyl alcohol. The deprotonation from the base alcohol in the cluster $ROH_2^+(H_2O)_n$ was not observed up to $n = 6$ or 7. The acid-catalyzed dehydration of alcohols was not observed either. The stepwise sums of free energy changes $\Delta G°_{n-1,n}$ for gas-phase hydration reactions of protonated alcohols and other ions are compared with the free energies of hydration. The anomalous order of basicities for H_2O and aliphatic alcohols is suggested in the gas phase and in aqueous solution. The sums of $\Delta G°_{n-1,n}$ for halide ions converge more gradually to the ultimate free energies of hydration than those for other positive ions.

There has been growing interest in the nature of cluster ions formed by the attachment of molecules to ions. This is due to the fact that the results contribute to a deeper understanding of the forces between ions and neutral molecules.[1] Furthermore, research in the cluster chemistry is very valuable for the elucidation of phenomena occurring in the condensed phase.[2]

Equilibria for the ion-solvent molecule clustering reactions involving positive or negative ions can be measured in the gas phase. The van't Hoff plots of the equilibrium constants lead to the determination of thermochemical data $\Delta G°$, $\Delta H°$, and $\Delta S°$ for the stepwise addition of solvent molecules to the ion. The present work reports the gas-phase equilibria measurements of the hydration reactions of protonated methyl alcohol, ethyl alcohol, n-propyl alcohol, and isopropyl alcohol. The obtained thermochemical data give some insight for the elucidation of ion hydration in the condensed phase.

Experiental Section

The measurements were made with the pulsed electron beam high-pressure mass spectrometer which has been described previously.[3,4]

Small amounts of CH_3OH, C_2H_5OH, n-C_3H_7OH, i-C_3H_7OH, and H_2O were introduced into ~4 Torr of CH_4 carrier gas through stainless steel capillaries. The pressure of alcohol was ≤1 mTorr. The equilibrium constants of hydration reactions of protonated alcohols were found to be independent on the change of H_2O pressure in the range 30-300 mTorr.

Results and Discussion

1. Hydration Reactions of Protonated Alcohols. Figure 1 shows the van't Hoff plots for the hydration reactions 1-4 of protonated methyl alcohol, ethyl alcohol, n-propyl alcohol, and isopropyl alcohol up to $n = 6$. The equilibrium constants below −40 °C

$$CH_3OH_2^+(H_2O)_{n-1} + H_2O = CH_3OH_2^+(H_2O)_n \quad (1)$$

$$C_2H_5OH_2^+(H_2O)_{n-1} + H_2O = C_2H_5OH_2^+(H_2O)_n \quad (2)$$

$$n\text{-}C_3H_7OH_2^+(H_2O)_{n-1} + H_2O = n\text{-}C_3H_7OH_2^+(H_2O)_n \quad (3)$$

$$i\text{-}C_3H_7OH_2^+(H_2O)_{n-1} + H_2O = i\text{-}C_3H_7OH_2^+(H_2O)_n \quad (4)$$

(i.e. $1000/T(K) < \sim 4.3$) could not be measured due to the

(1) Hiraoka, K.; Shoda, T.; Morise, K.; Yamabe, S.; Kawai, E.; Hirao, K. *J. Chem. Phys.* **1986**, *84*, 2091.
(2) Castleman, A. W., Jr. *Adv. Colloid Interface Sci.* **1979**, *10*, 73.
(3) Hiraoka, K.; Morise, K.; Shoda, T. *Int. J. Mass Spectrom. Ion Proc.* **1985**, *67*, 11.
(4) Hiraoka, K.; Morise, K.; Nishijima, T.; Nakamura, S.; Nakazato, M.; Ohkuma, K. *Int. J. Mass Spectrom. Ion Proc.* **1986**, *68*, 99.

0002-7863/86/1508-5683$01.50/0